Selective Photocleavage of DNA by Anthraquinone Derivatives: Targeting the Single-Strand Region of Hairpin Structures†

Paul T. Henderson, Bruce Armitage, and Gary B. Schuster*

School of Chemistry and Biochemistry, Georgia Institute of Technology, Atlanta, Georgia 30332-0400

Received September 30, 1997; Revised Manuscript Received December 18, 1997

ABSTRACT: A tetracationic anthraquinone derivative (27AQS2) binds to hairpin DNA and irradiation of the bound quinone leads to selective strand cleavage. NMR spectroscopy reveals that 27AQS2 binds at the loop and to the stem−loop junction of hairpin DNA. UV irradiation of the bound quinone causes cleavage of the DNA in the loop region and at guanines in the stem region. Inclusion of ethidium bromide in the reaction mixture leads to a greatly increased selectivity for loop cleavage. Spectroscopic and chemical evidence suggests a three component mechanism for reaction. The ability to target single-stranded regions of DNA structures is an important property of this photonuclease.

Recent advances in molecular biology have led to a need for new chemical tools for the detection, manipulation, and analysis of biologically important substances—particularly proteins and nucleic acids. Natural nucleases are enzymes that cleave single- or double-stranded DNA or RNA at specific locations. They are very useful, but their large size and limited sequence recognition capabilities prevents their general application. An area in which chemists have made substantial contributions is in the design and development of nucleases for use as structural probes and as therapeutic agents. One especially appealing class of artificial nucleases is the photonucleases (*1*). With a photonuclease, all components of the system to be studied can be assembled before the chemical reaction is initiated with light. The ability to control light, in both a spatial and temporal sense, is advantageous for applications that require the spatially or time-resolved analysis of a biochemical process or system. Another important feature of photonucleases is that light can be a very selective reagent. Activation of a properly chosen photonuclease can occur in the presence of other cofactors or enzymes.

A wide-range of photonucleases have been reported in the attempt to take advantage of their special properties and fulfill the needs of molecular biology (*2*). One class of photonuclease targets the hydrogen atoms of the deoxyribose groups of DNA. Generally, these compounds cleave DNA with no or low sequence selectivity. Their structures are quite varied: they may be metal-containing compounds such as uranyl acetate (*3*−*6*) and organometallic complexes of rhodium (*7*, *8*) cobalt (*9*−*11*) and platinum, (*12*−*13*), or organic compounds such as enediynes (*14*, *15*), nitro-substituted aromatics, (*16*, *17*) or halogen-containing compounds (*18*−*20*). A second class of photonuclease generates a diffusible intermediate that reacts with the nucleic acid to initiate strand cleavage. This class contains reagents that generate singlet oxygen (*21*−*23*) and hydroxyl radical (*24*). The former reacts selectively at guanine; the latter generally initiates nonselective cleavage of the DNA. A third class of photonuclease operates by single-electron transfer. This group includes riboflavin (*25*) and naphthalimide derivatives (*26*, *27*), organometallic compounds (*28*), and certain anthraquinone derivatives (*29*−*32*). Generally, a photonuclease in this class oxidizes a base to form the radical cation which may migrate until it is trapped at a GG step leading to preferential cleavage of the 5′-G of this sequence.

The wide-ranging properties and characteristics of existing photonucleases provide useful tools for the cleavage and analysis of DNA. One goal for the further development of photonucleases is the discovery of agents that cleave DNA in regions having unique structures. Our work in the development of anthraquinone derivatives as photonucleases is directed, in part, toward the fulfillment of this objective.

The anthraquinone photonucleases we have discovered to date cleave DNA by three distinct mechanisms that give three different cleavage patterns. Their mechanism of action is controlled by the mode of binding of the quinone to the DNA which, in turn, is determined by the structure of the quinone and by the composition of the buffer solution. For anthraquinones that bind to DNA by intercalation, irradiation leads to electron transfer and preferential damage to the 5′-G of GG steps which yields efficient strand cleavage only when the irradiation is followed by treatment with alkali (*29*, *31*). Irradiation of nonintercalated anthraquinones gives nonselective, spontaneous (no alkali treatment required) cleavage that presumably results from hydrogen atom abstraction from a deoxyribose (*30*). Irradiation of an anthraquinone unbound to DNA in chloride-containing solution gives extraordinarily efficient, nonselective, spontaneous cleavage of DNA that is useful in footprinting experiments (*33*).

To understand the effects that unusual nucleic acid structures may have on quinone binding and cleavage specificity, we chose to study the reaction of the octadeca-

† The financial support by the NIH (GM28190) is gratefully acknowledged. The NMR spectrometers used in this work were purchased with funds provided, in part, by the National Science Foundation Grant BIR-9306392.

S0006-2960(97)02419-7 CCC: $15.00
Published on Web 02/06/1998

Chart 1: Structures of Anthraquinone Derivatives and DNA Oligomers

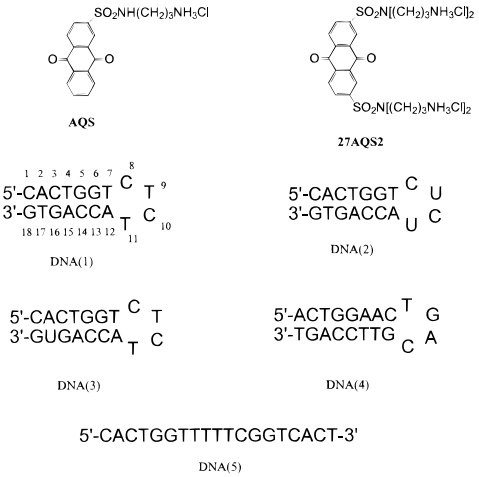

nucleotide DNA(1) with 27AQS2[1] (see Chart 1). DNA(1) belongs to a class of single-stranded DNA and RNA oligomers having partially self-complementary sequences that form stem−loop structures known as "hairpins" (*34*). DNA hairpins have been identified in trinucleotide repeats associated with human disease (*35*). The stem region of the hairpin is typically in a standard B-form structure that is bridged by the single-stranded loop. Two-dimensional NMR spectral analysis of through space and through bond connectivities using homonuclear chemical shift changes and peak broadening indicate that 27AQS2 binds to DNA(1) at the loop−stem junction and at the loop. We find also that irradiation of 27AQS2 under certain conditions results in cleavage of DNA(1) selectively in the single-stranded region. Experiments extended to a hairpin whose loop contains both pyrimidines and purines show that 27AQS2 is of general utility for the selective cleavage of loops in DNA hairpins.

MATERIALS AND METHODS

General. DNA(1) was prepared and purified by HPLC using standard solid-state synthetic methods. The other oligonucleotides used in this work were purchased from Midland Certified Reagent Company (anion exchange or gel filtration grade) or from GIBCO and used as received. Oligonucleotide concentrations were determined by absorbance at 260 nm. The Klenow fragment of DNA polymerase and T4 Polynucleotide kinase were purchased from New England Biolabs and used as received. Anthraquinone-2-sulfonate was purchased from Aldrich and used as received. AQS and 27AQS2 were synthesized according to previously published methods (*36*). [α-^{32}P]-dATP, dNTPs, and [γ-^{32}P]-ATP were purchased from Amersham and used as received. UV Spectra were recorded on a Cary-1E spectrophotometer. Phosphorescence emission spectra were measured on a Spexfluorolog spectrometer. NMR spectral characterization were carried out on a Bruker DRX 500 MHz instrument.

Preparation of Radiolabeled DNA. 3′-End-labeling reactions were performed using the Klenow fragment of DNA polymerase and [α-^{32}P]-dATP: A 250 pmol sample of DNA (DNA(4) truncated by three bases at the 3′ end to facilitate efficient labeling using the 5′ overhang as a template for the enzyme) was dissolved in 5.0 μL of [α-^{32}P]-dATP (3000 Ci/mmol) and 0.5 μL (2.5 units) of the Klenow fragment of DNA polymerase in a total volume of 20 μL, and the mixture was incubated for 15 min at room temperature. A series of 2.0 μL portions of unlabeled dNTP (1.0 μM in each deoxyoligonucleotide) was added, and the mixture was incubated for 5 min at room temperature and then warmed to 70 °C for 5 min to inactivate the enzyme. The DNA sample was suspended in denaturing loading buffer and purified on a 20% denaturing polyacrylamide gel. After autoradiography, the band corresponding to DNA(4) was excised from the gel and eluted in 350 μL of elution buffer (0.5 M NH_4OAc, 10 mM $Mg(OAc)_2$, 1.0 mM EDTA, and 0.1% SDS) at 37 °C for 4 h and centrifuged at 12 000 g for 5 min. The DNA was precipitated from the supernatant by addition of 3.0 μL of 10 mM $MgSO_4$, 5.0 μL of 3M NaOAc (pH = 5.2), and 700 μL of cold ethanol. The mixture was vortexed, placed on dry ice for 30 min, centrifuged at 12 000 g for 30 min, and the supernatant removed. The resulting pellets were washed three times with 80% ethanol.

5′-End-labeling reactions were performed using T4 Polynucleotide kinase and [γ-^{32}P]-dATP. A 250 pmol sample of DNA(1) was incubated with 5.0 μL of [γ-^{32}P]-ATP (6000 Ci/mmol) and 1.0 μL (8 units) of T4 Polynucleotide kinase in a total volume of 20 μL at 50 °C for 60 min. After incubation, the DNA was suspended in denaturing loading buffer and purified on a 20% denaturing polyacrylamide gel and eluted from the gel as described above.

Selected oligonucleotide samples were treated with 1 M piperidine at 90 °C for 30 min to elicit nonspontaneous cleavage. A+G, G, and T sequence markers were produced according to the Maxam−Gilbert sequencing protocol (*37*).

Photocleavage Experiments. Samples were prepared for irradiation by incubating labeled DNA (5000 cpm) with 5 or 10 μM of unlabeled DNA(1) in a 10 mM sodium phosphate buffer solution containing 5 or 10 μM of anthraquinone derivative and other components as indicated. For samples containing SOD (3 units) or catalase (4.8 units), the enzyme was added prior to irradiation. The sample volume was adjusted to 20 μL with water. For samples dissolved in D_2O, the appropriate aqueous components were combined and lyophilized to dryness prior to dissolution in D_2O. Samples were irradiated in 1.5 mL microcentrifuge tubes using a Rayonet photoreactor equipped with eight lamps (λ = 350 nm). The tubes were suspended from a rotating sample holder and cooled from below with a fan installed in the base of the photoreactor.

After irradiation, 35 μL of water, 5.0 μL of 3M NaOAc (pH = 5.3), 0.5 μL of $MgCl_2$, 1.0 M, 1.0 mL 500 μM (bp) of sonicated calf thymus DNA, and 100 μL of cold ethanol were added to the samples in the order indicated. The DNA was precipitated by incubation on dry ice for 30 min followed by centrifugation at 12 000 g for 30 min. The resulting pellets were washed twice with 100 μL of 80% ethanol, dried for 5 min at low heat by Speedvac (Savant Instruments), treated with piperidine if required, and dissolved in 5.0 μL of denaturing formamide loading buffer. The photocleavage products were separated by electrophoresis on a 20% polyacrylamide gel and detected by autoradiography.

[1] Abbreviations: EB, Ethidium bromide; AQS, N-(3-aminopropyl)-2-anthraquinonesulfonamide hydrochloride; AQS2, *N*,*N*,*N*′,*N*′-tetrakis-(3-aminopropyl)-2,7-anthraquinonesulfonamide tetrahydrochloride; SOD, superoxide dismutase; dAMP, deoxyadenosine monophosphate; dNTP, deoxyribonucleoside 5′-triphosphate.

UV−Vis Spectroscopy. Thermal denaturation studies were carried out in 1 cm path length semimicro cells by monitoring sample absorbance at 260 nm. A heating/cooling rate of 0.5 °C/min was maintained. Melting temperatures were determined from the maxima of first derivative plots.

Phosphorescence Quenching. Aqueous buffer solutions containing 30% ethylene glycol, 10 μM 27AQS2 and DNA-(1) and EB in NMR sample tubes were submerged in liquid nitrogen contained in an optical Dewar flask. The samples were excited at 330 nm and the phosphorescence emission spectra were recorded from 400 to 625 nm.

NMR Spectral Studies: DNA(1). A 5 mg sample of DNA-(1) was dissolved in 0.6 mL of a D_2O−10 mM sodium phosphate buffer solution (pH = 7). The samples were exchanged with D_2O by three successive cycles of evaporation followed by redissolution with 0.6 mL of D_2O. One-dimensional ^{1}H-NMR spectra were recorded on a Bruker DRX 500 MHz spectrometer on nonspinning sample into 32 K data points over a spectral width of 12 ppm. Each spectrum consisted of 32 transients with a 4 s recycle delay during which the HOD resonance was suppressed by low-power irradiation.

Phase-sensitive NOESY and COSY spectra were acquired in absorption mode utilizing time-proportional phase incrimentation (TPPI) (*38*). Phase cycling permitted quadrature detection in t_1, and the spectrometer carrier offset was placed at the water solvent resonance frequency. NOESY spectra of the samples in D_2O were recorded with a mixing time 350 ms. A continuous radio frequency irradiation was applied during the recycle delay and during the mixing time of the NOESY experiments to saturate the residual HOD resonance. All of the 2D-homonuclear experiments in D_2O were acquired with a spectral width of 10 ppm. In all experiments, the spectra were recorded with 512 increments in t_1 and 1024 complex points in t_2. For all spectra 32 transients were averaged for each t_1 value. The data were apodized in both dimensions with skewed sinebell squared filters. Zero filling of the data produced 2D matrix sizes of 1 × 4 K real points. The data were processed with the FELIX software package (Hare Research, Inc.) and with XWinn-Plot (Bruker, Inc.) running on a Silicon Graphics IRIS workstation.

RESULTS

(1) Association of 27AQS2 with Hairpin DNA−Melting Data. The partially self-complementary 18 mer, DNA(1) was designed to serve as a probe for analysis of the association and reactions of 27AQS2 with hairpin DNA. Examination of the melting behavior of DNA(1) by UV spectroscopy reveals one transition with $T_m = 54$ °C. These data are shown in Figure 1 in the form of first-derivative plots. We have previously shown that 27AQS2 binds to duplex DNA with an association constant that depends on sequence (*36*). With poly(dAdT)$_2$, K_a is ca. 10^6 M^{-1}; for poly(dGdC)$_2$, K_a is ca. 5×10^5 M^{-1}. Addition of 27AQS2 to DNA(1) causes stabilization of the hairpin, but the melting behavior of DNA(1) in the presence of 27AQS2 is complex. Addition of 1 equiv of the anthraquinone results in the appearance of at least two apparent phase transitions. The first has $T_m \approx 62$ °C and the second at ≈78 °C. The lower temperature transition disappears as more 27AQS2 is added to the solution. When the ratio of 27AQS2 to DNA(1) is 4:1, only a single transition with $T_m \approx 81$ °C is observed. These findings indicate that there are at least two different modes for binding 27AQS2 to DNA(1). The first, with the higher apparent binding constant, results in less stabilization of the hairpin than the second. In contrast, addition of AQS (see Chart 1) to a DNA(1) solution results in only a single melting transition with $T_m = 60$ °C over the entire concentration range examined. AQS normally binds to duplex DNA by intercalation.

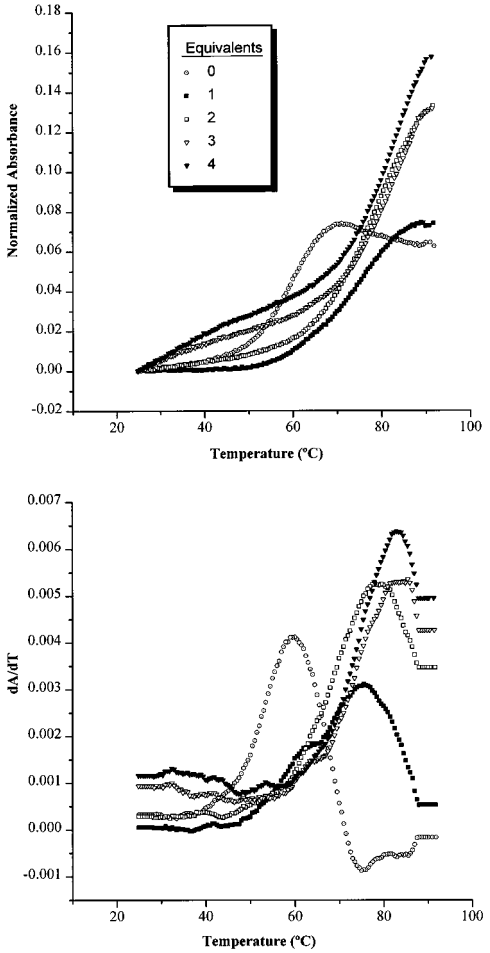

FIGURE 1: Melting curves (left panel) and first derivative plots (right panel) for additions of 0−4 equiv of 27AQS2 to DNA(1), 10 μM, monitored at 260 nm in phosphate buffered solution.

(2) Association of 27AQS2 with Hairpin DNA−NMR Spectroscopy. The objectives of the NMR spectral analysis are to confirm helix formation for the stem portion of DNA-(1) and to identify the binding sites of 27AQS2 with the hairpin. These objectives were accomplished by substitutions of uracils for thymines, by application of 2D-spectroscopic techniques, and by "titration" of DNA(1) with 27AQS2.

Figure 2 shows the portion of the 1D-NMR spectrum for DNA(1) from $\delta = 1.4-1.9$ which contains the expected five methyl group resonances for the thymines. Also shown in Figure 2 are the spectra of two other DNA oligomers that were prepared to aid the assignment of the T-methyl (T-Me) peaks of DNA(1). In DNA(2), T_9 and T_{11}, two bases expected to be in the loop region, were replaced by uracil (U). In DNA(3), T_{17} is replaced by U. Since U differs from T only by the absence of a methyl group in the former, comparison of the spectra in Figure 2 permits the assignment

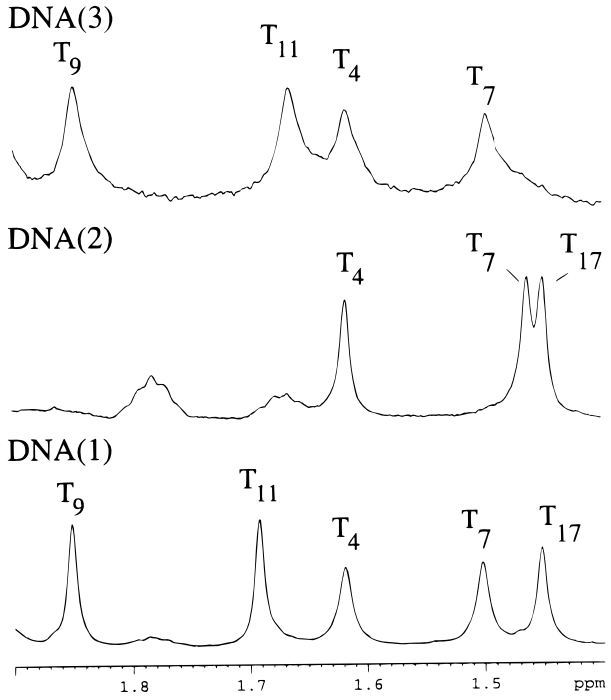

FIGURE 2: 1D-^{1}H NMR spectra of DNA(1), DNA(2), and DNA-(3) showing the T-methyl region ($\delta = 1.4-1.9$) at room temperature in phosphate buffered D_2O.

Table 1: Proton Chemical Shifts for DNA(1) Assigned by U Substitution and COSY and NOESY Spectroscopy

	proton chemical shifts[a]						
residue	CH_8	CH_6	CH_5	T-methyl	$H_{1'}$	$H_{2'}$	$H_{2''}$
C_1		7.87	6.00		6.08	2.96	2.83
A_2	8.41				5.72	1.97	2.43
C_3		7.40	5.33		6.25	2.25	2.40
T_4		7.31		1.63	5.93	2.00	2.52
G_5	7.86				5.72	2.07	2.43
G_6	7.73				5.72	2.72	2.78
T_7		7.28		1.51	6.00	2.52	2.74
C_8		7.73	6.08		6.25	2.53	2.20
T_9		7.56		1.87	6.08	2.12	2.26
C_{10}		7.42	6.07		5.83	2.13	2.25
T_{11}		7.37		1.70	5.89	2.20	1.98
A_{12}	8.41				6.26	2.84	2.95
C_{13}		7.37	5.33		5.33	2.83	2.95
C_{14}		7.50	5.61		5.90	2.07	2.43
A_{15}	8.26				5.47	2.07	2.40
G_{16}	7.71				6.08	2.95	2.83
T_{17}		7.16		1.46	5.91	2.39	1.94
G_{18}	7.93				6.18	2.62	2.40

[a] All chemical shifts are reported in ppm (δ) referenced to TMS.

of methyl resonances for T_9, T_{11} ($\delta = 1.87$ or 1.70), and T_{17} ($\delta = 1.46$) of DNA(1). Replacement of T_9 and T_{11} with uridines causes the chemical shift of only one of the three remaining methyl groups to change from that of the unmodified hairpin. The affected resonance is assigned to T_7 ($\delta = 1.51$) on the basis of its location at the stem−loop junction. These assignments of the resonances for the T-methyl groups are refined further by analysis of 2D-^{1}H NMR spectra of DNA(1) These experiments are described in the Appendix. The assigned chemical shifts are shown in Table 1.

A major objective of the NMR spectral analysis of DNA-(1) is assessment of the binding locations for 27AQS2. We found that the T-Me proton chemical shifts are sensitive measures of binding by the quinone. Five aliquots of

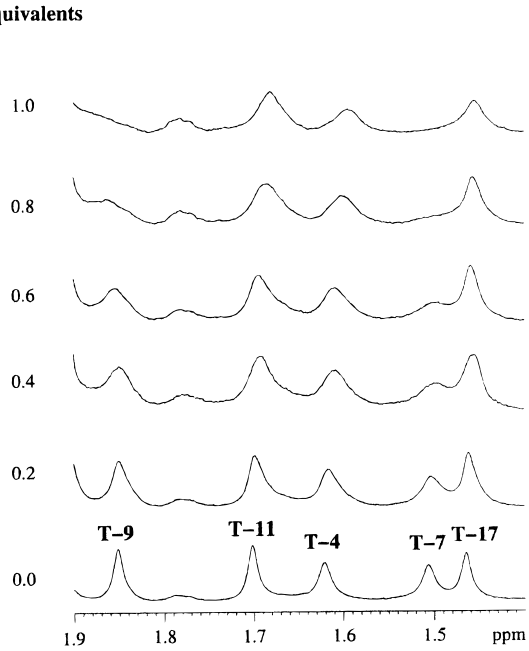

FIGURE 3: Titration of DNA(1) with 27AQS2, added in 0.2 equiv aliquots, monitored by ^{1}H-NMR spectroscopy $\delta = 1.4-1.9$ (T-methyl region) in phosphate-buffered D_2O at 10 °C.

27AQS2, each corresponding to 0.2 equiv, were added sequentially to a solution of DNA(1). After each addition, the spectrum of the T-Me region was recorded from 5 to 25 °C in 5 °C increments. Figure 3 shows the effect of this "titration" on DNA(1) with 27AQS2 at 10 °C. Clearly, all of the T-Me group resonances are broadened by the addition 27AQS2. This indicates an intermediate rate of exchange, which is consistent with our earlier stopped-flow measurements for dissociation of 27AQS2 from duplex DNA. The T-Me peaks are not affected equally by addition of the quinone. For example, T_{17} and T_4, located in the stem region, are virtually unaffected by addition of the first two aliquots of 27AQS2, but T_7, located at the stem−loop junction, is severely broadened and shifted by the first additions of the quinone. Similarly, T_9, which is in the loop region of DNA-(1), is broadened and shifted as the amount of 27AQS2 in solution is increased. To a lesser extent T_{11}, also in the loop region, broadens and shifts slightly as the concentration of quinone is increased. These findings indicate that there are multiple binding sites for the quinone that differ only slightly in their association constants. However, there appears to be a clear preference for association of the quinone at the stem−loop junction and in the loop region of the hairpin. This finding is consistent with the complex melting behavior which was described above.

(3) Photocleavage of DNA(1) with 27AQS2. We previously showed that irradiation of 27AQS2 causes alkali-requiring, essentially nonselective cleavage (slightly higher efficiency at G and GG steps) of duplex DNA (*36*). We examined the light-induced cleavage of DNA(1) by 27AQS2 under a variety of conditions to probe its ability to discriminate between the single-stranded loop and the duplex stem of this hairpin structure. The photochemistry of AQS, which binds by intercalation to duplex DNA, was examined for comparison.

Irradiations of chloride-free phosphate buffer solutions (pH = 7.0) of 27AQS2 or AQS and 1 equiv of DNA(1), including

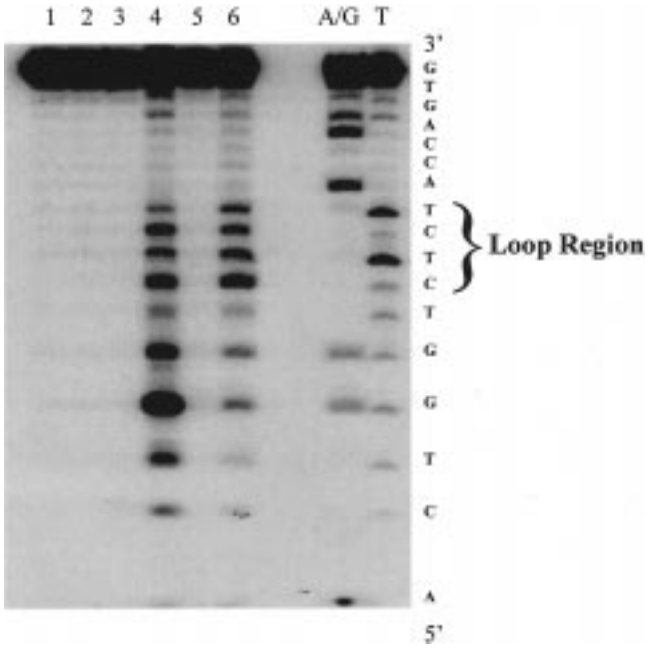

FIGURE 4: Autoradiogram of irradiated (350 nm, 30 °C) samples of DNA(1), 10 μM, with 1 equiv of AQS or 27AQS2. Lane 1 is an unirradiated control sample with no quinone or piperidine treatment. Lane 2 is the same as lane 1 but treated with piperidine at 90 °C for 30 min. Lane 3 is an irradiated AQS-containing sample with no piperidine treatment. Lane 4 is an irradiated AQS sample that has been treated with piperidine. Lane 5 is the same as lane 3 with 27AQS2. Lane 6 is the same as lane 4 with 27AQS2. Lanes marked A/G and T are Maxam−Gilbert sequencing lanes.

a portion which had been 5′-^{32}P-end-labeled, were carried out in a Rayonet photoreactor (8 lamps, 350 nm, 2 h) and were monitored by polyacrylamide gel electrophoresis (PAGE) and autoradiography. The results, shown in Figure 4, indicate that irradiation of either 27AQS2 or AQS gives little spontaneous cleavage of DNA(1). However, treatment of the irradiated AQS solutions with piperidine causes cleavage in the stem region at the G_5G_6 step (predominately at G_5, the 5′-G) and at each of the bases in the loop region with T_{11} apparently less efficiently cleaved than the other loop bases. Treatment of the irradiated 27AQS2 sample with piperidine reveals strong cleavage at each of the loop bases and weaker cleavage at the G_5G_6 step. Clearly, both AQS and 27AQS2 can cleave the single-stranded region of DNA-(1). However, 27AQS2 appears to be more selective in this ability, and it appears that the loop bases are cleaved more uniformly with this quinone.

We previously reported that inclusion of Cl^- in solutions of anthraquinones changes the mechanism of reaction for DNA cleavage (*33*). For example, irradiation of anthraquinone-2-sulfonate (AQSO) in the presence of Cl^- gives nonselective cleavage that does not require piperidine treatment. Irradiation of 27AQS2 in a solution containing 100 mM NaCl does not change the need for piperidine treatment, but it does cause a significant change in the cleavage pattern for DNA(1). The relative amount of cleavage at the guanines in the stem increases in the presence of Cl^-. The inclusion of Cl^- also increases the apparent reaction efficiency since shorter irradiation times give equivalent amounts of cleavage when Cl^- is present. These observations are helpful in the analysis of the reaction mechanism.

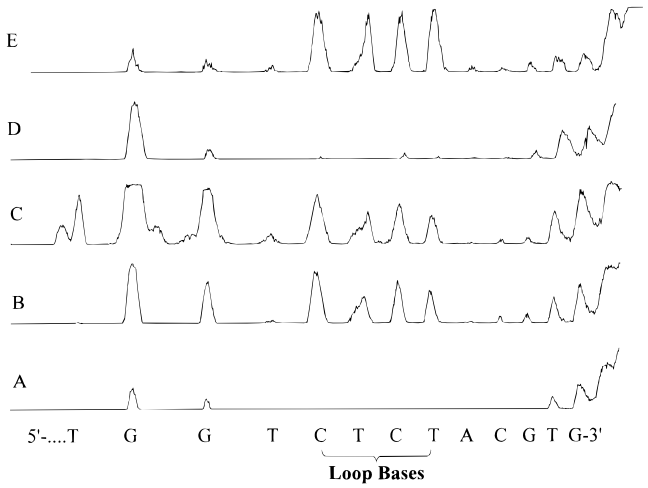

FIGURE 5: Histogram showing: (A) background (dark control) cleavage of DNA(1), 5 μM in phosphate buffered H_2O with 100 mM NaCl, in the presence of 1 equiv of 27AQS2 after piperidine treatment; (B) same as A but after 30 min of irradiation; (C) same as B except that D_2O replaces H_2O; (D) same as B except that 50 mM dAMP was added before irradiation; (E) same as B except that 4 equiv of EB were added before irradiation.

Adenine is predicted to quench the triplet state of 27AQS2 by electron transfer (*39*) at approximately the diffusion-limited rate. We examined the ability of deoxyadenosine monophosphate (dAMP) to quench the cleavage from irradiation of 27AQS2 in the presence of the hairpin. Quenching would indicate that the excited quinone is accessible from solution since dAMP bears negative charge and is not expected to associate with DNA. Irradiation of 27AQS2 in the presence of 50 μM dAMP and DNA(1) results in a significant reduction of loop cleavage and a relative increase in the cleavage at the 5′-G of the GG step (Figure 5). The effect is not due to an increase in ionic strength, since an equivalent amount of $NaClO_4$ has no effect on the cleavage efficiency. It is clear that some, but not all, of the sites of bound 27AQS2 are accessible to dAMP, and the 27AQS2 at sites not accessible to dAMP induce cleavage that resembles that of an intercalated quinone.

One objective of the present investigation is the design of a system that will selectively cleave hairpin DNA in the single-stranded region. The experiments with 27AQS2 described above reveal considerable promise toward attainment of this objective. However, cleavage at the GG step in the stem region of the hairpin also occurs. In related systems, we find that the anthraquinone triplet excited-state oxidizes a base in the duplex region of the DNA and that the resulting radical cation migrates to a GG step where it is trapped yielding, eventually, cleavage at this site (*31*). We carried out photocleavage experiments in the presence of ethidium bromide (EB) in an attempt to increase selectivity and to probe the mechanism of the reaction of 27AQS2 with DNA(1) by inhibiting radical cation-initiated processes. Figure 5 shows a histogram that reveals the effect of including 4 equiv of EB in a chloride-free solution of 27AQS2 and DNA(1). Irradiation in the absence of EB gives cleavage in the loop region and at the GG step. The inclusion of EB has little effect on the loop cleavage but the GG cleavage in the stem is significantly inhibited.

Many anthraquinone derivatives phosphoresce in frozen solution. Since diffusion does not occur under these condi-

tions, quenching indicates preassociation of the quinone and its quencher. DNA effectively quenches the quinone phosphorescence when they are associated (*30*). The phosphorescence of 27AQS2 is nearly completely quenched by 0.25 equiv (with respect to 27AQS2) of DNA(1), thus indicating binding of the quinone. Significantly, addition of 0.5 equiv of EB to this mixture causes an increase in the emission to 29% of the free quinone. The effect of EB on the cleavage selectivity of 27AQS2 must be related to its ability to intercalate in duplex DNA. Binding of EB causes the release of some quinone and a base radical cation cannot migrate past an intercalated EB (E_{ox} of EB is 1.68 V vs NHE) (*40*).

Studies of other light-induced DNA cleaving agents have identified singlet oxygen ($^1O_2$), and superoxide ($O_2^{\bullet-}$) (*21*−*23*) as reagents capable of damaging DNA. We carried out a series of experiments to assess the role that $^1O_2$ and $O_2^{\bullet-}$ play in the 27AQS2 induced cleavage of DNA(1).

The lifetime of $^1O_2$ increases ca. 10-fold when the reaction solvent is changed from H_2O to D_2O (*41*). This effect has been used to verify the participation of $^1O_2$ in reactions with DNA since the increase in lifetime is manifested as a more efficient reaction (*42*). We compared the relative efficiency of cleavage observed from irradiation of 27AQS2 in Cl^- containing H_2O and D_2O solutions of DNA(1). The data, Figure 5, show that there is an increase in stem cleavage, particularly at the 5′G of the GG step, in the D_2O solution. These findings indicate that $^1O_2$ initiated cleavage occurs in the presence of Cl^-, and that it appears predominantly in the GG step of the stem region of DNA(1). In an experiment to probe for a role for $O_2^{\bullet-}$, we showed that the light-induced cleavage is not inhibited when superoxide dismutase (SOD, 3 units) and/or catalase (4.8 units) are added to the reaction mixture (*43*). These findings indicate that conversion of $O_2^{\bullet-}$ to hydroxyl radicals through hydrogen peroxide does not play a significant role in the cleavage process.

The loop region of DNA(1) has only pyrimidine bases. We prepared and examined DNA(4) which contains each of the four DNA bases in the loop, see Chart 1, to determine if the selective cleavage observed with 27AQS2 extends to purines. Irradiation of 27AQS2 in a phosphate buffered solution containing 100 mM NaCl and 1 equiv of DNA(4) results in nearly equally efficient cleavage of each of the four bases in the loop as well as cleavage of the G at the stem−loop junction and less efficient cleavage at other guanines, Figure 6. Irradiation of chloride-containing solutions of quinone and DNA gives nonselective spontaneous background cleavage (*33*). This is seen in lane 3 of Figure 6. Clearly, 27AQS2 is capable of cleaving both purines and pyrimidines in the loop region of hairpin DNA.

(4) Photocleavage of Single-Stranded DNA with 27AQS2. The alkali-requiring cleavage of both purines and pyrimidines in the loop region of DNA(1) by 27AQS2 is unusual. Oxidative damage of DNA typically accumulates at guanines, and hydrogen atom abstraction from a deoxyribose usually results in spontaneous cleavage of the DNA (*2*). We examined the photochemistry of 27AQS2 in the presence of single-stranded DNA to assess the generality of this alkali-dependent, nonselective cleavage.

Irradiation of 27AQS2 in chloride-free phosphate buffer solution in the presence of DNA(5), see Chart 1, gives only a small amount of spontaneous cleavage. However, treatment of the irradiated sample with piperidine results in

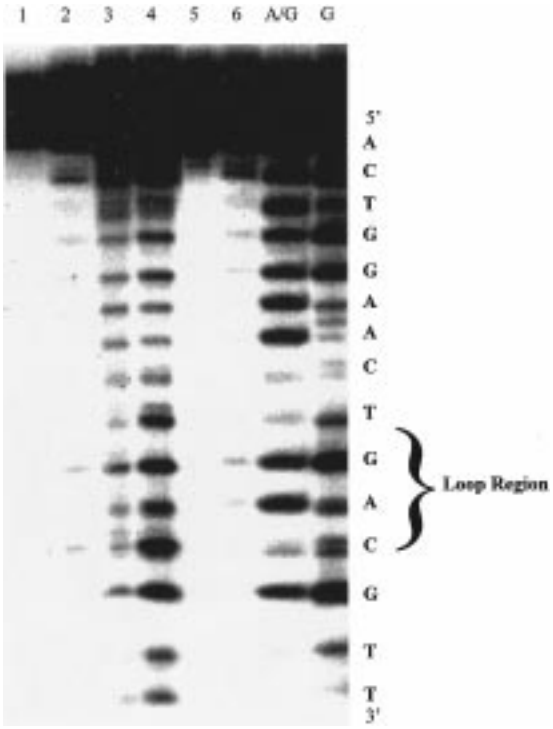

FIGURE 6: Autoradiogram of irradiated (350 nm, 30 °C) samples of DNA(4), 10 μM, with 1 equiv of 27AQS2 in Cl^- containing phosphate buffer solution. Lane 1 is an unirradiated control sample with quinone and without piperidine treatment. Lanes 5 and 6 are irradiated samples of DNA(4) without and with piperidine treatment, respectively (no 27AQS2). Lane 2 is the same as lane 1 but treated with piperidine at 90 °C for 30 min. Lane 3 is an irradiated 27AQS2-containing sample with no piperidine treatment. Lane 4 is an irradiated 27AQS2 sample that has been treated with piperidine. Lanes marked A/G and G are Maxam−Gilbert sequencing lanes.

cleavage at each base, the data are shown in Figure 7. Both purines and pyrimidines are cleaved, but the cleavage efficiency is not uniform. Certain guanines and thymines are cleaved with higher apparent yield than are other bases. This may be a consequence of limited access to certain bases in the random coil structure of the single-stranded DNA, or it may be due to a reduced ability of a radical cation to migrate in a single-stranded structure. Regardless, this result provides additional evidence useful for analysis of the reaction mechanism of 27AQS2 with DNA(1).

DISCUSSION

(1) Binding of 27AQS2 to DNA(1). Both the melting behavior experiments and the NMR spectral analysis indicate that the binding of 27AQS2 to DNA(1) is complex. There is no single binding site that is preferred strongly over others. This is revealed by multiple transitions in the melting profile as the amount of quinone is increased and by the effect of 27AQS2 on the NMR spectrum of DNA(1).

We have shown previously that the binding mode of anthraquinone derivatives having ammonium group-containing side chains is strongly dependent on structural details (*32*). In most cases, monocationic derivatives intercalate, but this is not universally so. In the case of 27AQS2, analysis of its interaction with the Dickerson−Drew dodecamer by NMR spectroscopy suggests that it binds to duplex DNA in the minor groove at AT-rich regions (*36*). The

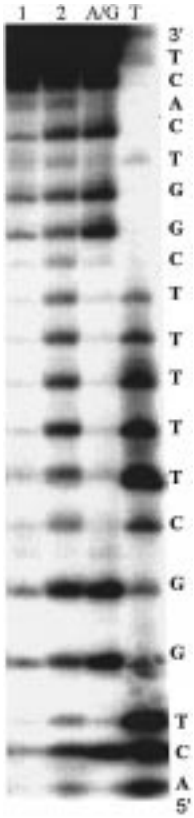

FIGURE 7: Autoradiogram from irradiation of DNA(5), 5 μM with 1 equiv of 27AQS2 in phosphate buffered solution. Lane 1 is the dark control after treatment with piperidine. Lane 2 is the same as lane 1 but after 2 h of irradiation. Lanes marked A/G and T are Maxam−Gilbert sequencing reactions.

NMR spectra of DNA(1) in the presence of 27AQS2 shows perturbation in the T-Me resonances at the stem−loop junction and in the loop. Thus there is little doubt that the quinone interacts with the bases in these regions. We suspect that this interaction is dominated primarily by electrostatic and hydrophobic interactions, but further work is required to develop a more refined picture.

The binding of 27AQS2 to DNA(1) is only one factor that affects the nature of its light-induced cleavage reaction. We have previously shown that radical cations ("holes") can migrate over a considerable distance in duplex DNA (*44*). Thus the cleavage at G_5 and G_6 of DNA(1) by 27AQS2 does not require the quinone to be bound near this GG step. Oxidation of a base in any portion of this structure could introduce a hole that is trapped at this site. Our examination of the 27AQS2 induced cleavage was designed, in part, to assess the mechanism of this reaction.

(2) Photocleavage of Hairpin DNA by 27AQS2. Irradiation of 27AQS2 results in at least three processes that cause cleavage of DNA(1). The first gives cleavage of bases in the loop that does not involve $^1O_2$: it is enhanced by the presence of Cl^-, strongly quenched by dAMP, and it is not very sensitive to EB. The second gives cleavage in the stem at the GG step, primarily the 5′-G: it, too, does not involve $^1O_2$, it is less sensitive to quenching by dAMP than loop cleavage, but it is strongly inhibited by EB. The third process also gives GG cleavage in the stem and it is significantly enhanced when the solvent is changed from H_2O to D_2O. On the basis of this observation this process is attributed to the reaction of DNA(1) with $^1O_2$.

Irradiation of 27AQS2 at 350 nm gives its singlet excited state. The singlet state may react with the DNA or intersystem cross to give the triplet excited state. Intersystem crossing in anthraquinone derivatives substituted with electron withdrawing groups (i.e., those having lowest energy nπ* triplet states) occurs in less than 10 ps (*45*). Our previous examination of the reactions of anthraquinone derivatives with duplex DNA indicated no (or, at most, a minor amount) cleavage originating from the singlet excited state. We presume that this is the case, too, for the reaction of 27AQS2 with DNA(1). Consequently, the three processes identified above are assigned to reactions originating with the triplet of 27AQS2. Rapid formation of the triplet in good yield is one of the features that makes anthraquinone derivatives especially useful for the cleavage of DNA.

Singlet oxygen generation is generally understood to result from energy transfer from the triplet state of a sensitizer (27AQS2 in this case) to molecular oxygen (*21*−*23*). There have been several examinations of the reaction of $^1O_2$ with DNA that identify guanines as the preferred site of reaction. In this regard, there is nothing remarkable about the $^1O_2$-dependent cleavage of DNA(1) except for the effect of Cl^-. Addition of Cl^- to the reaction solution enhances the amount of cleavage caused by $^1O_2$. We attribute this to an effect of the increased ionic strength of the Chloride-containing solution. At the higher ionic strength, there is more unbound 27AQS2, and it is this species that will be most effective as a sensitizer.

The loop cleavage and the non-$^1O_2$ stem cleavage are attributed to related reaction mechanisms. In both cases the triplet of 27AQS2 may oxidize a base to its radical cation or abstract a hydrogen atom from a deoxyribose. It has been shown that base radical cations will migrate in duplex DNA to GG steps where alkali-requiring cleavage occurs preferentially at the 5′-G (*28*, *44*, *46*). We previously showed that oxidation to form base radical cations occurs efficiently from intercalated quinones, but NMR and other spectral analyses indicate that 27AQS2 generally does not intercalate in duplex DNA. Consequently, there appears to be a binding mode unique to the hairpin structure of DNA(1) that permits oxidation of a base to its radical cation or hydrogen atom abstraction. The NMR spectral analysis of 27AQS2 and DNA(1) shows that one site for binding is the stem−loop junction. We suggest that quinone triplet state bound there can oxidize a base and that the resulting radical cation may migrate to the GG step in the stem. Support for this hypothesis comes from the experiments with dAMP and EB which show that stem and loop cleavage originate, at least in part, from quinones bound to different sites of DNA(1). dAMP quenches loop cleavage more effectively than it quenches cleavage in the stem. On this basis we conclude that 27AQS2 leading to stem cleavage is at a binding site that is less accessible from solution. Similarly, inhibition of stem cleavage by EB indicates selective quinone displacement or that intercalated EB imposes an insurmountable barrier to migration of the radical cation. Thus 27AQS2 responsible for stem cleavage must be capable of introducing a radical cation into the stem. 27AQS2 bound at the stem−loop junction appears to fulfill both of these requirements. Clearly, however, certain identification of the precise structure of the reactive complex will require additional data.

Cleavage in the loop region of DNA(1) may also be a consequence of reaction by a quinone bound at the stem−loop junction, or it may be caused by 27AQS2 bound to the loop itself. Support for a role for the latter binding mode also comes from the NMR data and the differential quenching of stem and loop cleavage by dAMP. We presume that 27AQS2 bound to the single-stranded loop of DNA(1) is more accessible to dAMP than quinone bound at the stem−loop junction. This will result in more quenching of the stem cleavage by dAMP if only the quinone bound at the junction can introduce a radical cation into the stem.

The damage, and subsequent cleavage, of a base other than guanine by an oxidative (radical cation) process is unusual (*2*). However, it is important to recall that the cleavage selectivity observed in this process is a consequence of the competition between migration of the radical cation and its trapping by water or oxygen. If the rate of migration in the single-stranded region is comparable to or slower than the rate of reaction of a base radical cation with water or oxygen, then the selectivity for G-cleavage will be lost. This view is supported by the cleavage initiated by irradiation of 27AQS2 with single-stranded DNA(5) which reveals cleavage at each of the four DNA bases. With the available data, we cannot distinguish between retardation of migration and acceleration of trapping, but either, or both, seem possible and likely. Alternatively, cleavage in the loop might be a consequence of hydrogen atom abstraction by selectively bound triplet quinone.

The effect of Cl^- on the efficiency of cleavage may be explained within the mechanistic hypothesis just discussed. The triplet state of 27AQS2 is a strong enough oxidant to convert each of the four DNA bases to its radical cation or to oxidize Cl^- to the chlorine atom. Formation of atomic chlorine by an unbound quinone results in the spontaneous, nonselective cleavage of duplex DNA by a process attributed to hydrogen atom abstraction from a deoxyribose. We suggest that the chlorine atom generated by oxidation with 27AQS2 bound in the single strand region of DNA(1) will, in turn, oxidize a base to its radical cation. The bases are more accessible in the single-stranded region than in duplex DNA, and consequently, exothermic electron transfer to the chlorine atom can become faster than hydrogen atom abstraction. This suggested mechanism accommodates the need for alkali treatment to cause cleavage even in the Cl^- containing solutions. Alternatively, the chlorine atom might abstract a hydrogen atom from a deoxyribose unit.

CONCLUSIONS

The anthraquinone derivatives 27AQS2 and AQS bind differently to the hairpin structure of DNA(1) than they do with duplex DNA. The consequences of the change in binding mode are particularly apparent for 27AQS2. Spectroscopic analysis and melting temperature behavior reveal multiple binding sites for 27AQS2 with DNA(1). One of these sites is assigned to the stem−loop junction, another is assigned to the single-stranded loop. Irradiation of 27AQS2 in the presence of DNA(1) initiates three processes that result in strand cleavage. One is $^1O_2$ generation which causes cleavage at guanines. A second is oxidation of a base in the stem to its radical cation which causes selective cleavage at the 5′-G of its GG step. The third is reaction of a base or sugar in the loop which leads to nonselective cleavage of the single strand of the hairpin. Cleavage of the loop can be made the nearly exclusive reaction from 27AQS2 by the inclusion of EB in the reaction mixture. Thus 27AQS2 has unique properties which may be valuable in applications for the determination of complex structures containing single stranded regions in DNA and RNA.

ACKNOWLEDGMENT

We thank Dr. Nadia Boguslavsky for synthesis of DNA(1) and Tina Davis and Dr. Leslie Gelbaum for expert advice and technical assistance with the NMR spectroscopy. We thank Professor W. David Wilson of Georgia State University for helpful discussions and assistance.

APPENDIX

COSY spectral coupling connectivities and NOESY spectral distance relationships were analyzed to yield the nonexchangeable base and sugar proton assignments for DNA(1) in a D_2O solution containing 10 mM Na_2PO_4 at pH 7.0 and 25 °C (*47*).

The COSY spectrum of DNA(1) is shown in Figure 8. The general identification of spectral regions corresponding to particular types of protons is readily assigned by the strong groupings of cross peaks (*48*). The pyrimidine bases are identified by the off-diagonal cross peaks of the aromatic protons. In DNA, the only scalar-coupled protons are the CH_5 and CH_6 of cytosine (part A). Consequently, the five strong cross peaks in the aromatic region clearly identify the CH_5 and CH_6 protons of the six cytosines in the sequence, with two of the cross peaks overlapping. The weaker cross peaks connecting the 7 ppm region to the 1 ppm region (part B) are the result of four-bond coupling between methyl and CH_6 protons and serve to identify the protons of the five thymine residues. Thus the six cytosine and five thymine residues are identified through the COSY spectrum. Vicinal proton coupling connectivities between sugar $H_{1'}$ protons ($\delta = 5.3-6.3$) and the sugar $H_{2'}$, $H_{2''}$ protons ($\delta = 1.8-3.0$) allow the assignment of some sugar protons that are ambiguous in the NOESY spectra due to excessive overlap of the sugar proton cross peaks (data not shown). The results of the COSY experiment confirm the nonexchangeable base and sugar ring proton assignments based on the NOESY data.

Figure 9 (part A) shows the expanded NOESY plots used to establish distance connectivities from the base protons ($\delta = 7.0-8.6$) to the sugar $H_{1'}$ and cytidine CH_5 protons ($\delta = 5.0-6.4$), and (part B) to the methyl protons ($\delta = 1.2-2.0$). The purine CH_8 and pyrimidine CH_6 base protons exhibit NOE cross peaks to their own and to the 5′-flanking sugar $H_{1'}$ protons in the duplex region of the hairpin and, to a lesser extent, in the loop region (*49*, *50*).

The thymine methyl resonance at $\delta = 1.62$ in the NOESY spectrum of Figure 9 part B is a convenient starting point for the sequential assignments. This resonance cross saturates its own CH_6 at $\delta = 7.31$ as well as the cytosine CH_6 resonance at $\delta = 7.40$. The only cytosine-thymine (CT) step in the duplex region of the hairpin is C_3T_4. The CT steps in the loop region of DNA(1) do not give strong aromatic proton to methyl group cross peaks, which further supports the assignment of the C_3T_4 step.

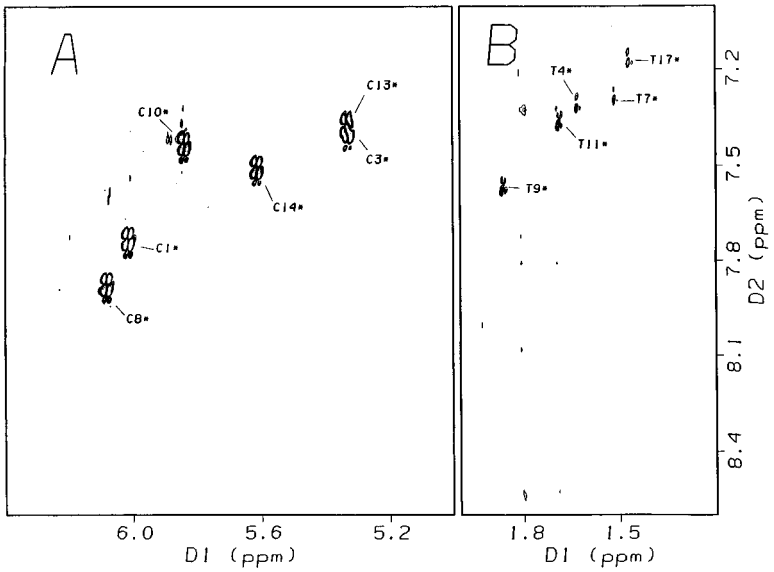

FIGURE 8: COSY spectrum of DNA(1) at 25 °C in phosphate buffered D_2O showing scalar couplings between (A) cytidine CH_5 and CH_6 resonances and (B) thymine methyl group and CH_6 resonances.

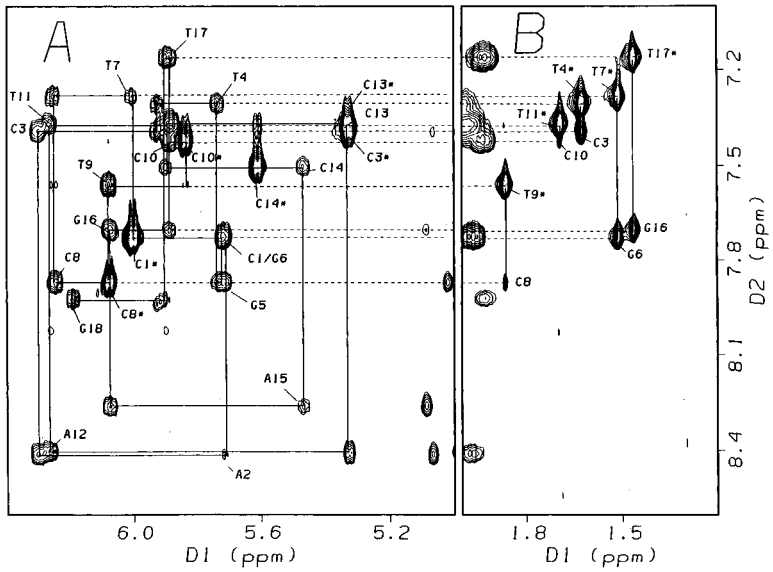

FIGURE 9: Phase-sensitive NOESY spectrum of DNA(1) at 25 °C in phosphate buffered D_2O solution collected with a mixing time of 350 ms. The expansion of the region marked A is the aromatic proton to $H_{1'}$ and H_5 cross peaks. The expansion of the region marked B is the aromatic proton to T-methyl cross peaks. The dotted lines indicate connectivities with aromatic proton chemical shifts common to both the $H_{1'}$ and T-methyl regions. The solid lines indicate sequential connectivities between proton resonances within the same spectral region.

The linkage of a CH_6 thymine resonance to the methyl group resonance of that thymine is revealed through the weak four-bond scalar coupling with that methyl group (Figure 3, part B). Thus the aromatic proton at $\delta = 7.31$ is CH_6 of T_4. In the aromatic $CH_5 \times H_{1'}$ region (part A), there are two $H_{1'}$ cross peaks to $\delta = 7.31$. The one at $\delta = 5.35$ also cross saturates the C_3 CH_6 proton. This peak is assigned to C_3 $H_{1'}$ since, in turn, it cross saturates a $H_{1'}$ resonance at $\delta = 6.31$ whose chemical shift corresponds to a singlet in the 1D-^{1}H NMR spectrum. This singlet has no COSY cross peaks, so it must be a purine. This resonance also weakly cross saturates to a cytosine at $\delta = 6.02$ with an aromatic proton at $\delta = 7.74$. Since there is only one purine in DNA-(1) between two cytosines, these resonances must be assigned to A_2 and C_1. The A_2 $CH_8 \times C_1$ $H_{1'}$ cross peak is weak either because the terminal deoxyribose ring assumes a different conformation from those in the interior of the helix, or to the effects of motion (fraying) (*48*).

Applying similar logic, and moving in the 3′ direction from T_4, allows assignment of the $H_{1'}$ and aromatic protons of the G_5G_6 step. The G_5 intra- and interresidue cross peaks of GH_8 and $H_{1'}$ and one of the G_6 $H_{1'}$ cross peaks to GH_8 are coincident. These G_5G_6 cross peaks are separated by their GH_8 chemical shifts ($\delta = 7.89$ and 7.75, respectively). The assignment of the G_5G_6 step was verified by the CH_8 cross peak (*47*) between the two guanines and by the CH_8 cross peaks with $H_{2'}$ and $H_{2''}$ cross connectivities (data not shown). This assignment strategy was successfully applied to the entire hairpin, with cross peaks in the loop showing different intensities than those in the stem. The aromatic proton intraresidue cross peaks present throughout the duplex region (except between C_1 and A_2) are absent in the loop

bases. These assignments, and those made similarly, are summarized in Table 1.

The formation of a right-handed helix for the stem of DNA(1) in aqueous solution is reflected in the observed directionality of the intrastrand NOE between base protons and their own and 5′- flanking $H_{1'}$ and $H_{2'}$, $H_{2''}$ protons (*51*). The base to sugar $H_{1'}$ NOE cross peaks are much weaker than the CH_5 to CH_6 cytidine NOE cross peaks (fixed 2.45 Å separation) consistent with all nucleotides adopting anti-glycosidic torsion angles along the length of the hairpin oligonucleotide (*48*).

The pattern and relative intensities of the cross peaks between the base and H1′ protons for nucleotides 1−7 and nucleotides 11−18 of the hairpin indicate that the stem region of DNA(1) forms a regular right-handed helical structure. Although a complete proton chemical shift assignment using the standard strategy for B-form DNA is not possible due to overlap of the cross peaks from the stem and the loop regions, analysis of the internucleotide NOE, at least, permits assignment of the T-Me protons and sequential assignment of the stem and loop bases.

REFERENCES

1. Kochevar, I. E., and Dunn, D. A. (1990) *Bioorg. Photochem. 1*.
2. Armitage, B. (1998) *Chem. Rev.* (Submitted for publication).
3. Nielsen, P. E., Jeppesen, C., and Buchardt, O. (1988) *FEBS Lett. 235*, 122.
4. Nielsen, P. E., Mollegard, N. E., and Jeppesen, C. (1990) *Anti-Cancer Drug Des. 5*, 105.
5. Mollegard, N. E., Murchie, A. I. H., Killey, D. M. J., and Nielsen, P. E. (1994) *EMBO J 13*.
6. Nielsen, P. E. (1992) *Nucleic Acids Res. 17*, 2735.
7. Chow, C. S., and Barton, J. K. (1992) *Methods Enzymol. 212*, 219.
8. Sitlani, A., Long, E. C., Pyle, A. M., and Barton, J. K. (1992) *J. Am. Chem. Soc. 114*, 2303−2312.
9. Chang, C.-H., and Meares, C. F. (1982) *Biochemistry 21*, 6332.
10. Saito, I., Morii, T., Sugiyanma, H., Matsuura, T., Meares, C. F., and Hecht, S. M. (1989) *J. Am. Chem. Soc. 111*, 2307.
11. Riordan, C. G., and Wei, P. (1994) *J. Am. Chem. Soc. 116*, 2189.
12. Kalsbeck, W. A., Gingell, D. M., Malinsky, J. E., and Thorp, H. H. (1994) *J. Am. Chem. Soc. 116*, 3313.
13. Breiner, K. M., Daugherty, M. A., Oas, T. G., and Thorp, H. H. (1995) *J. Am Chem. Soc. 117*, 11673.
14. Shiraki, T., and Sugiura, Y. (1990) *Biochemistry 29*, 9795.
15. Wender, P. A., Zercher, C. K., Beckham, S., and Haubold, E. M. (1993) *J. Org. Chem. 58*, 5867.
16. Nielsen, P. E., Jeppesen, C., Egholm, M., and Buchardt, O. (1988) *Biochemistry 27*, 6338.
17. Kuroda, R., Satoh, H., Shinomiya, M., Watanbe, T., and Otuska, M. (1995) *Nucleic Acids Res. 23*, 1524.
18. Matsumoto, T., Sakai, Y., Toyooka, K., and Shibuya, M. (1992) *Heterocycles 33*, 135.
19. Quada, J. C., Jr., Levy, M. J., and Hecht, S. M. (1993) *J. Am. Chem. Soc. 115*, 12171.
20. Chen, T., Voelk, E., Platz, M. S., and Goodrich, R. P. (1996) *Photochem. Photobiol. 64*, 622.
21. Cadet, J., and Teoule, R. (1978) *Photochem. Photobiol. 28*, 661.
22. Kawanishi, S., Inoue, S., and Sano, S. (1986) *J. Biol. Chem. 261*, 6090.
23. Lee, P. C. C., and Rogers, M. A. (1987) *Photochem. Photobiol. 45*, 79.
24. MacGregor, R. B. J. (1992) *Anal. Biochem. 204*, 324.
25. Ito, K., Inoue, S., Yamamoto, K., and Kawanishi, S. (1993) *J. Biol. Chem. 268*, 13221−13227.
26. Saito, I., Takayama, M., and Kawanishi, S. (1995) *J. Am. Chem. Soc. 117*, 5590−5591.
27. Saito, I., Takayama, M., Sugiyama, H., Nakatani, K., Tsuchida, A., and Yamamoto, M. (1995) *J. Am. Chem. Soc. 117*, 6406−6407.
28. Hall, D. B., Holmlin, R. E., and Barton, J. K. (1996) *Nature 382*, 731−735.
29. Armitage, B. A., Yu, C., Devadoss, C., and Schuster, G. B. (1994) *J. Am. Chem. Soc. 116*, 9847−9859.
30. Breslin, D. T., and Schuster, G. B. (1996) *J. Am. Chem. Soc. 118*, 2311−2319.
31. Ly, D., Kan, Y., Armitage, B., and Schuster, G. B. (1996) *J. Am. Chem. Soc. 118*, 8747−8748.
32. Breslin, D. T., Coury, J. E., Anderson, J. R., McFail-Isom, L., Kan, Y., Williams, L. D., Bottomley, L. A., and Schuster, G. B. (1997) *J. Am. Chem. Soc. 119*, 5043−5044.
33. Armitage, B., and Schuster, G. B. (1997) *Photochem. Photobiol. 66*, 164-170.
34. Hilbers, C. W., Haasnoot, C. A. G., de Bruin, S. H., Joordens, J. J. M., Van Der Marel, G. A., and Van Boom, J. H. (1985) *Biochimie 67*, 685−695.
35. Mitas, M. (1997) *Nucleic Acids Res. 25*, 2245−2253.
36. Breslin, D. T., Yu, C., Ly, D., and Schuster, G. B. (1997) *Biochemistry* (In press).
37. Sambrook, J., Fritsch, E. F., and Maniatis, T. (1989) *Molecular Cloning. A Laboratory Manual* Cold Spring Harbor Press, Cold Spring Harbor, NY.
38. Marion, D., and Wuthrich, K. (1983) *Bichem. Biophys. Res. Commun. 113*, 967−974.
39. Steenken, S., and Jovanovic, S. V. (1997) *J. Am. Chem. Soc. 119*, 617−618.
40. Fromherz, P., and Rieger, B. (1986) *J. Am. Chem. Soc. 108*, 5361−5362.
41. Rogers, M. A. J., and Snowden, P. T. (1982) *J. Am. Chem. Soc. 104*, 5541−5543.
42. Showen, K. B., and Showen, R. L. (1982) *Solvent Isotope Effects on Enzyme Systems* Academic Press, New York.
43. Hertzberg, R. P., and Dervan, P. B. (1982) *J. Am. Chem. Soc. 102*, 313−315.
44. Gasper, S. M., and Schuster, G. B. (1998) *J. Am. Chem. Soc.* (in press).
45. Moore, J. N., Phillips, D., Nakashima, N., and Yoshihara, K. (1987) *J. Chem. Soc., Faraday Trans. 2 83*, 1487−1508.
46. Arkin, M. R., Stemp, E. D., Pulver, S. C., and Barton, J. K. (1997) *Chem., and Biology 4*, 389−400.
47. Wuthrich, K. (1986) *NMR of Proteins and Nucleic Acids* John Wiley and Sons, New York.
48. Hare, D. R., Wemmer, D. E., Chou, S. H., Drobny, G., and Reid, B. R. (1983) *J. Mol. Biol. 171*, 319−336.
49. Scheek, R. M., Boelens, R., Russo, N., van Boom, J. H., and Kaptein, R. (1984) *Biochemistry 23*, 1371−1376.
50. Hare, D. R., and Reid, B. R. (1986) *Biochemistry 25*, 5341−5350.
51. Feigon, J., Leupin, W., Denny, W. A., and Kearns, D. R. (1983) *Biochemistry 22*, 5943−5951.

BI972419G